REPORT

Mutations in *CEP78* Cause Cone-Rod Dystrophy and Hearing Loss Associated with Primary-Cilia Defects

Konstantinos Nikopoulos,[1,12] Pietro Farinelli,[1,12] Basilio Giangreco,[2] Chrysanthi Tsika,[3] Beryl Royer-Bertrand,[1,4] Martial K. Mbefo,[5] Nicola Bedoni,[1] Ulrika Kjellström,[6] Ikram El Zaoui,[1] Silvio Alessandro Di Gioia,[1] Sara Balzano,[1] Katarina Cisarova,[1] Andrea Messina,[7] Sarah Decembrini,[5] Sotiris Plainis,[3] Styliani V. Blazaki,[3] Muhammad Imran Khan,[8] Shazia Micheal,[8] Karsten Boldt,[9] Marius Ueffing,[9] Alexandre P. Moulin,[10] Frans P.M. Cremers,[8,11] Ronald Roepman,[8] Yvan Arsenijevic,[5] Miltiadis K. Tsilimbaris,[3] Sten Andréasson,[6] and Carlo Rivolta[1,*]

Cone-rod degeneration (CRD) belongs to the disease spectrum of retinal degenerations, a group of hereditary disorders characterized by an extreme clinical and genetic heterogeneity. It mainly differentiates from other retinal dystrophies, and in particular from the more frequent disease retinitis pigmentosa, because cone photoreceptors degenerate at a higher rate than rod photoreceptors, causing severe deficiency of central vision. After exome analysis of a cohort of individuals with CRD, we identified biallelic mutations in the orphan gene *CEP78* in three subjects from two families: one from Greece and another from Sweden. The Greek subject, from the island of Crete, was homozygous for the c.499+1G>T (IVS3+1G>T) mutation in intron 3. The Swedish subjects, two siblings, were compound heterozygotes for the nearby mutation c.499+5G>A (IVS3+5G>A) and for the frameshift-causing variant c.633delC (p.Trp212Glyfs*18). In addition to CRD, these three individuals had hearing loss or hearing deficit. Immunostaining highlighted the presence of CEP78 in the inner segments of retinal photoreceptors, predominantly of cones, and at the base of the primary cilium of fibroblasts. Interaction studies also showed that CEP78 binds to FAM161A, another ciliary protein associated with retinal degeneration. Finally, analysis of skin fibroblasts derived from affected individuals revealed abnormal ciliary morphology, as compared to that of control cells. Altogether, our data strongly suggest that mutations in *CEP78* cause a previously undescribed clinical entity of a ciliary nature characterized by blindness and deafness but clearly distinct from Usher syndrome, a condition for which visual impairment is due to retinitis pigmentosa.

Cone-rod degeneration (CRD [MIM: 120970]) represents an extremely rare class of hereditary diseases that affect the light-sensing neurons of the retina, the cone and rod photoreceptors.[1] Cones are involved in daytime vision, providing the brain with color information and central, precise visual input. Conversely, rods are active in very dim light conditions, are more abundant in the retinal periphery, and produce achromatic information, typical for instance of the visual stimulation provided by a landscape on a moonless night. Individuals with CRD experience initial loss of visual acuity (central vision) and aberrant color vision as a result of the prominent loss of cones, whereas rod functions remain relatively preserved.[2] As the disease progresses, both cone and rod functions deteriorate and central vision is severely impaired or lost, but peripheral islands of the retina might retain some residual activity.[3] On the basis of these clinical parameters, CRD can be distinguished from retinitis pigmentosa (RP [MIM: 26800], also called rod-cone degeneration), the most common form of hereditary retinal degeneration. In retinitis pigmentosa, rods are more severely affected than cones; initial symptoms include night blindness due to loss of rod function, and central vision (cone function) is often preserved until the very late stages of the disease.[4] CRD is almost invariantly inherited as a Mendelian trait, predominantly according to a recessive pattern of transmission, and is characterized by an elevated genetic and allelic heterogeneity.[5] Although as many as 33 CRD-associated genes have been identified to date (RetNet; see Web Resources), they are found to be mutated in only ~25% of clinical cases, implying that a substantial percentage of affected people might carry mutations in yet-to-be-identified genes.[6]

According to this rationale, we performed whole-exome sequencing (WES) in 34 unrelated individuals with CRD (29 from Greece and five from Sweden). Genomic DNA was extracted from peripheral blood leukocytes according to standard procedures, and then exomic libraries (SureSelect V5 kit, Agilent) were sequenced on an Illumina HiSeq 2000. Raw sequence files were assessed, trimmed, and finally mapped back to the human genome reference sequence (build hg19); DNA variants were called

[1]Department of Computational Biology, Unit of Medical Genetics, University of Lausanne, 1011 Lausanne, Switzerland; [2]Center for Psychiatric Neuroscience, Department of Psychiatry, Lausanne University Hospital, 1008 Lausanne, Switzerland; [3]Department of Ophthalmology, Medical School, University of Crete, 71003 Heraklion, Greece; [4]Center for Molecular Diseases, Lausanne University Hospital, 1011 Lausanne, Switzerland; [5]Unit of Gene Therapy and Stem Cell Biology, Jules Gonin Ophthalmic Hospital, 1004 Lausanne, Switzerland; [6]Lund University, Skane University Hospital, Department of Ophthalmology, 20502 Lund, Sweden; [7]Service of Endocrinology, Diabetes and Metabolism, Lausanne University Hospital, 1011 Lausanne, Switzerland; [8]Department of Human Genetics and Radboud Institute for Molecular Life Sciences, Radboud University Medical Center, 6525GA Nijmegen, The Netherlands; [9]Medical Proteome Center, Institute for Ophthalmic Research, University of Tuebingen, 72074 Tuebingen, Germany; [10]Department of Ophthalmology, Jules Gonin Ophthalmic Hospital, 1004 Lausanne, Switzerland; [11]Donders Center for Neuroscience, Radboud University, 6525EN Nijmegen, The Netherlands
[12]These authors contributed equally to this work
*Correspondence: carlo.rivolta@unil.ch
http://dx.doi.org/10.1016/j.ajhg.2016.07.009.

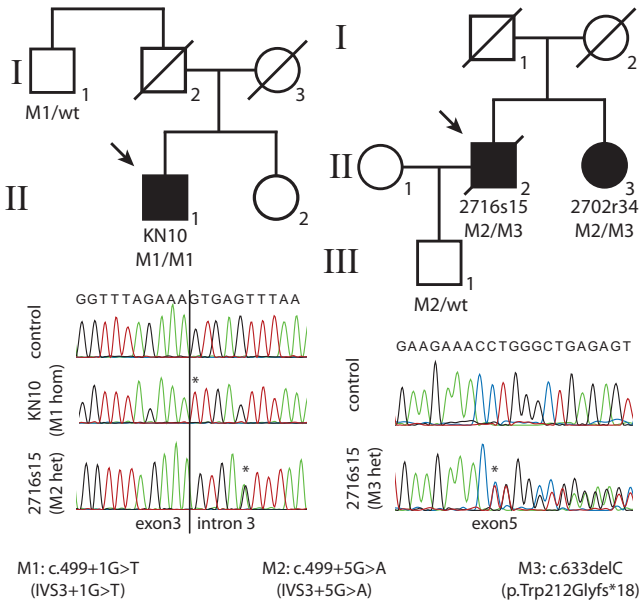

Figure 1. *CEP78* Mutations
Pedigrees and electropherograms of the identified DNA changes. Asterisks indicate the site of mutations. Abbreviations are as follows: Mx, mutant alleles; wt, wild-type allele.

and scored according to a specific in silico pipeline, described previously.[7] Aggregate data analysis and variant filtering procedures (Tables S1 and S2 in the Supplemental Data available online) revealed biallelic mutations in two probands, one from Greece and another from Sweden, in *CEP78* (centrosomal protein 78, composed of 16 exons for its longest coding isoform [GenBank: NM_001098802.1]). Both had classical signs and symptoms of CRD, clearly distinct from retinitis pigmentosa, as detailed below. Written informed consent was obtained from all individuals enrolled in this study, and approval for research on human subjects was obtained from the institutional review boards of all participating Institutions.

The Greek subject (KN10, individual II-1 on the left pedigree in Figure 1) was a 59-year-old male from the island of Crete and the eldest of two siblings of a non-consanguineous family. His sister was unaffected, and the family reported no history of retinal degeneration. Clinical history indicated hemarelopia since early adulthood (18–20 years of age); the condition progressed to severe central vision loss at the age of 35–40 years and evolved into severe visual impairment, nystagmus, and photophobia. Dyschromatopsia was also reported. Fundus examination at first visit showed normal color and normal vessels but a small atrophic foveal area with subjacent ring-like glistening in one eye and bull's-eye maculopathy in the other eye. A few atrophic lesions were present in the inferior periphery in one eye (Figure 2). The 30° static automated perimetry revealed a diffuse suppression of the visual field in both eyes and a relative conservation of the peripapillary and superior periphery. Full-field electroretinography (ERG) showed flat cone responses but still some residual rod-mediated signals in the left eye. This person also complained about minor hearing problems, and his audiogram exhibited relatively mild deficit; nonetheless, such deficit was clearly distinct and more severe than natural age-related hearing loss (presbycusis)[9] (Figure 2). KN10 carried a homozygous substitution in the first invariant base of intron 3 splice donor site c.499+1G>T (IVS3+1G>T) (Figure 1). This variant was located within a very small stretch of homozygosity that was not statistically significant for autozygosity, possibly indicating a mutational founder effect of geographic origin (not shown). The only relative who could be tested was his paternal uncle (individual I-1, left pedigree), who carried this DNA change heterozygously (Figure 1).

The Swedish proband (2716s15, individual II-2 on the right pedigree in Figure 1), now deceased, was last examined at 69 years of age. He was born from unaffected parents and was the first child of a kindred of two. His sister (2702r34, individual II-3, right pedigree), examined at age 65, also had retinal degeneration. Both had visual problems, including loss of color sensitivity and central vision, since childhood. Both also reported a hearing deficit since they were young, and both had hearing aids. Audiogram of the living Swedish subject at age 66 years revealed substantial sensorineural hearing loss, which did not seem to progress substantially over the following 11 years (Figure 2). Hospital records containing information on the hearing status of her deceased brother were destroyed upon his death. Fundus examination showed degenerative changes for both siblings in the macular region and some spicular pigment in the mid-periphery but fewer changes in the periphery (Figure 2). Progressive deterioration of the visual field was reported and documented as expanding from the center to the periphery. At last examinations, both siblings retained some residual vision at the periphery of the visual field, especially in dim-light conditions. Similar to the situation for the Greek subject, full-field ERG of both individuals highlighted almost no residual cone activity but still revealed some rod-mediated responses, even at these late ages. These siblings were compound heterozygotes for two *CEP78* mutations: a frameshift-causing single-nucleotide deletion (c.633delC; p.Trp212Glyfs*18) in exon 5 and an intronic base substitution (c.499+5G>A; IVS3+5G>A) in the vicinity of the donor site for intron 3, just four nucleotides away from the mutation identified in the Greek subject. Genetic examination of the proband's son (individual III-1, right pedigree) uncovered the presence of this latter mutation in heterozygosis, confirming the biallelic nature of the changes detected in his father and his aunt (Figure 1).

Sanger sequencing of the entire reading frame of *CEP78* in a cohort of 99 unrelated CRD-affected individuals of Swedish, Swiss, Dutch, and Pakistani ethnic background failed to identify any additional causative variants. The three mutations present in our two families were not detected in the genome of an internal control cohort of 350 unrelated individuals or in any other public

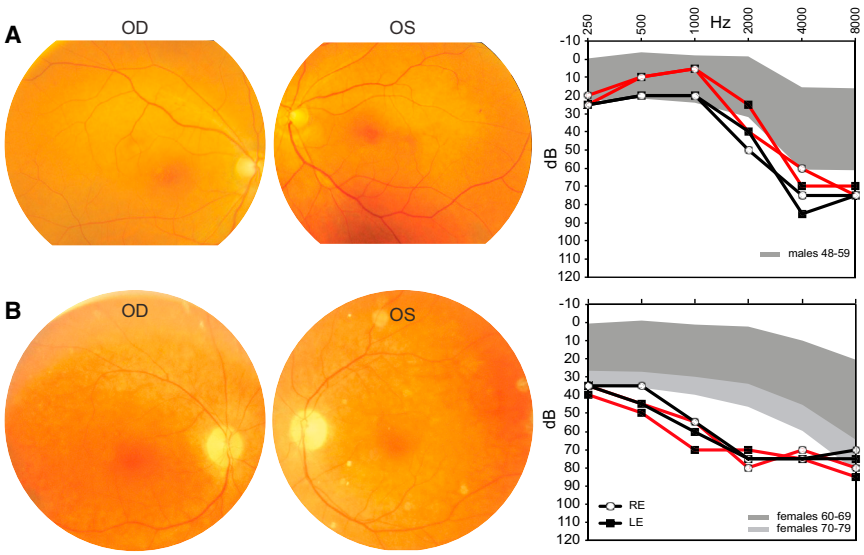

Figure 2. Clinical Features of the Analyzed Subjects

(A) Individual KN10. Fundus pictures (at age 53 years) reveal macular coalescent hypochromatic lesions in the right eye and minor macular changes in the left eye. Pure tone audiograms at age 57 years (black lines) and 59 years (red lines) show mild hearing impairment at higher frequencies compared to the normal range for gender and age, indicated by the shaded area.[8]

(B) Individual 2702r34. Fundus examination at age 65 years highlights attenuated vessels and degenerative changes in the posterior pole. Audiograms at age 66 years (black lines) and 77 years (red lines) show clear hearing loss at most frequencies. Abbreviations are as follows: OD, right eye; OS, left eye; RE, right ear; and LE, left ear.

database, including the 1000 Genomes Project, the Exome Variant Server (EVS), and the Exome Aggregation Consortium (ExAC) Browser, which reports sequencing data from more than 61,000 unrelated individuals. In addition, in silico assessment of the c.499+1G>T and c.499+5G>A mutations via two distinct web-based platforms, NNSPLICE 0.9[10] and Human Splicing Finder,[11] predicted for both variants the abolishment of the donor splicing site for intron 3.

To analyze the functional consequences of the three mutations, we obtained fresh blood samples and skin biopsies from the Greek proband and the living Swedish subject and performed the following experiments. We first retrotranscribed total RNA from immortalized lymphoblasts (GoScript Reverse Transcriptase, Promega). Then, after performing saturating RT-PCR of the region spanning all mutations (primers: 5′-TTTTGCAGAAGTCGTGTTCCT-3′ and 5′-TTCAAGGGCCTCTAGCAAAG-3′), we cloned the amplified products in *E. coli* (Zero Blunt PCR Cloning Kits, Invitrogen) and performed colony PCRs and capillary electrophoresis on 96 clones (48 clones per affected individual). Representative samples were Sanger sequenced, and relative numbers of splicing events were assessed and quantified. The c.499+1G>T mutation resulted invariantly in the skipping of exon 3, leading to the production of an aberrant isoform, never reported in genomic databases, for which exons 2 and 4 were joined together. This event ablated 24 codons and altered the reading frame of *CEP78*, leading to the formation of a premature termination codon at nucleotides 16–18 of exon 4. Therefore, this non-canonical transcript was predicted to trigger nonsense-mediated mRNA decay (NMD)[12] and result in no viable mRNA. The same exon-skipping occurrence was observed for the other, nearby mutation, c.499+5G>A, that was present in the Swedish subjects. Finally, the frameshift mutation c.633delC resulted in reduced mRNA amounts, as deduced by the low number of *E. coli* colonies carrying this cDNA clone (4 out of 48), again, probably as a result of the action of NMD. Immunoblot analysis in fibroblasts' extracts (antibodies: A301-799A, Bethyl Laboratories, epitope between residues 550 and 600 and A2066, Sigma, for beta actin) revealed the presence of CEP78 in very reduced amounts in the Greek subject and the absence of any detectable band in the Swedish subject, in agreement with the mRNA findings described above (Figure 3). More specifically, the homozygous c.499+1G>T mutation probably resulted in a few canonical mRNA forms not detected by our cloning experiments, in turn producing small amounts of CEP78. Concerning the Swedish subject, it is likely that both the c.633delC and the c.499+5G>A alleles produced mostly non-viable mRNA and minimal quantities of wild-type mRNA and protein. In fact, overexposed films showed a faint band corresponding to CEP78, indicating that the protein was present in trace amounts (not shown).

To gain insights into the relationship between vision and *CEP78*, we analyzed its expression in a panel of human tissues of cadaveric origin (Human Total RNA Master Panel II, Takara, primers 5′-GTTTCCCATTAATCAAAACACG-3′ and 5′-TCAACTTCAGAGGATGAAGGACT-3′ for *CEP78* and 5′-AGAGTGGTGCTGAGGATTGG-3′ and 5′-CCCTC ATGCTCTAGCGTGTC-3′ for the housekeeping gene *GUSB*). Although the number of *CEP78* transcripts in the retina was higher than in many other tissues and organs, retinal *CEP78* mRNA did not display the highest expression level (Figure 4). A time-course experiment on eyes of developing and postnatal mice (primers 5′-CTTCAGA AAGTGTCCAGGAAGC-3′ and 5′-GATCACTCTCTCCTCC TTCAGC-3′ for *Cep78* and 5′-CCTAAGATGAGCGCAAGTT GAA-3′ and 5′-CCACAGGACTAGAACACCTGCTAA-3′ for the housekeeping gene *Hprt1*) revealed high expression at embryonic stages, followed by a progressive decrease at perinatal stages and by a plateau at adulthood (Figure 4). This pattern is reminiscent of the expression of other genes involved in retinal degenerations and in early biogenesis and homeostasis of the centriole, notably

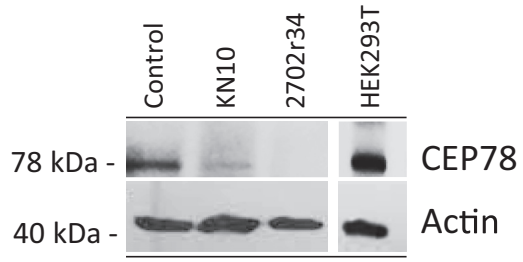

Figure 3. Immunoblot Analysis of Endogenous CEP78 in Fibroblasts from Affected Individuals
Numbers on the left refer to molecular-size markers. *Control* indicates human fibroblasts from a control individual; *HEK293T* indicates HEK293 cells containing SV40 large T antigen as a control for specificity of the anti-CEP78 antibody.

CEP76, *CEP110*, *CEP164* (MIM: 614848), *RAB8A* (MIM: 165040), *BBS4* (MIM: 600374), and *RPGR* (MIM: 312610).[13] Although we could not obtain primary data on *CEP78* expression in human cochlea, we assessed its RNaseq values from the only comprehensive transcriptome repository currently available for the inner ear.[14] *CEP78* displayed a FPKM (fragments per kilobase of exon per million reads mapped) value of 4.53 (average from three human cochleae), indicating moderate expression in this structure. Importantly, this FPKM value for *CEP78* appeared to be higher than that of most genes already known to be associated with hereditary deafness (40 out of 70, or 57%), as assessed in the same organs and in the same conditions (Table S3).

Little is known about the function of CEP78. Identified as a component of the centrosome by two independent proteomic screenings,[15,16] CEP78 is composed of five leucine-rich repeats located at the N-terminal half of the protein, as well as a coiled-coil domain at the C terminus. An important study using *Planaria* as the main experimental model revealed that miRNA-based knockdown of *CEP78* resulted in defective primary cilia assembly in flatworms and human RPE1 cells.[17] Intriguingly, *CEP78* was also found upregulated more than 5-fold by noise stress in rat cochlea.[18] The function and impact of CEP78 in human physiology, however, remain largely elusive.

The reported centrosomal localization of CEP78 prompted us to investigate a possible role in relationship to the photoreceptor primary cilium. Immunofluorescence of human retinal sections with anti-CEP78 antibody (IHC-00364, Bethyl Laboratories, epitope between residues 550 and 600) and anti-cone arrestin (SC-54355, Santa Cruz) showed that CEP78 is present in dot-shaped foci in the inner segments, probably at the base of the primary cilium in retinal photoreceptors, predominantly cones (Figure 5 and Figure S1). This observation was confirmed when CEP78 was labeled together with acetylated tubulin, staining the primary cilium of human skin fibroblasts (Figure 5). Interestingly, positive staining was observed in fibroblasts from KN10 and 2702r34 as well, confirming that *CEP78* was in fact expressed at the protein level in these individuals, as inferred (Figure 5). The mild differences between these experiments and the protein-expression observations might be due to different sensitivities of the two analytical tools and the use of distinct antibodies (A301-799A for immunoblot and IHC-00364 for immunofluorescence). No specific differences concerning CEP78 subcellular localization were observed in cells from affected individuals versus cells from controls.

Presence at the base of the connecting cilium is a characteristic that is shared by other proteins associated with retinal degeneration, and in particular by FAM161A, the deficiency of which causes the RP28 form of retinitis pigmentosa (MIM: 606068).[19–21] Indeed, tandem-affinity purification analysis performed with full-length FAM161A showed a positive interaction with CEP78,[22] and co-immunoprecipitation with an anti-CEP78 antibody (A301-800A, Bethyl Laboratories, epitope between residues 639 and

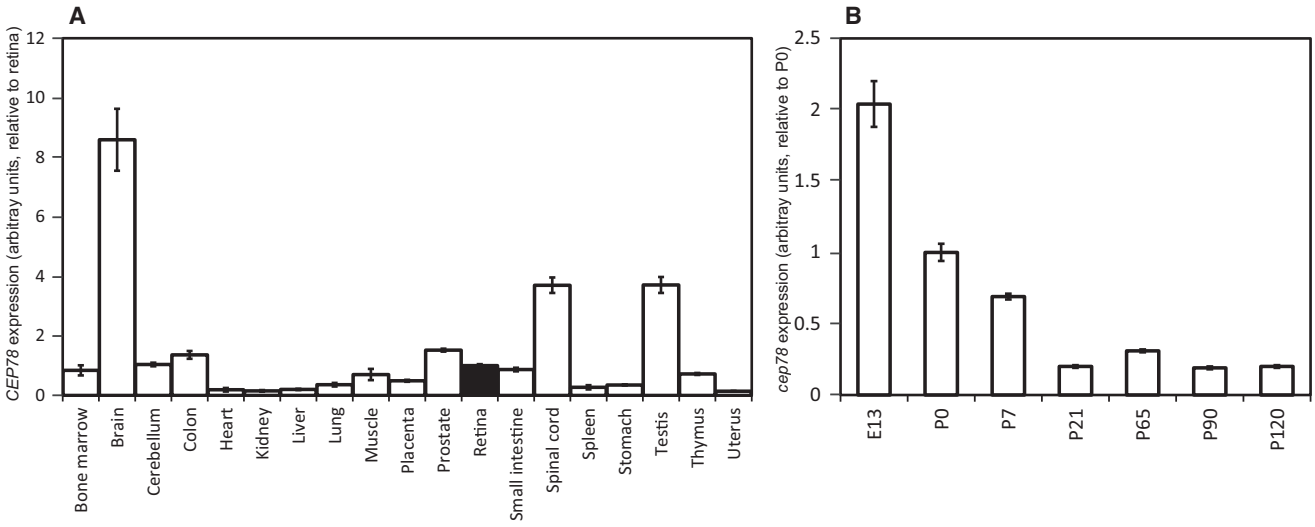

Figure 4. *CEP78* mRNA Expression in Various Human Tissues and Organs and in the Developing Murine Eye
Data are from real-time PCR relative expression analysis, for which *GUSB* and *Hprt1* were used as normalizing genes for (A) and (B), respectively.

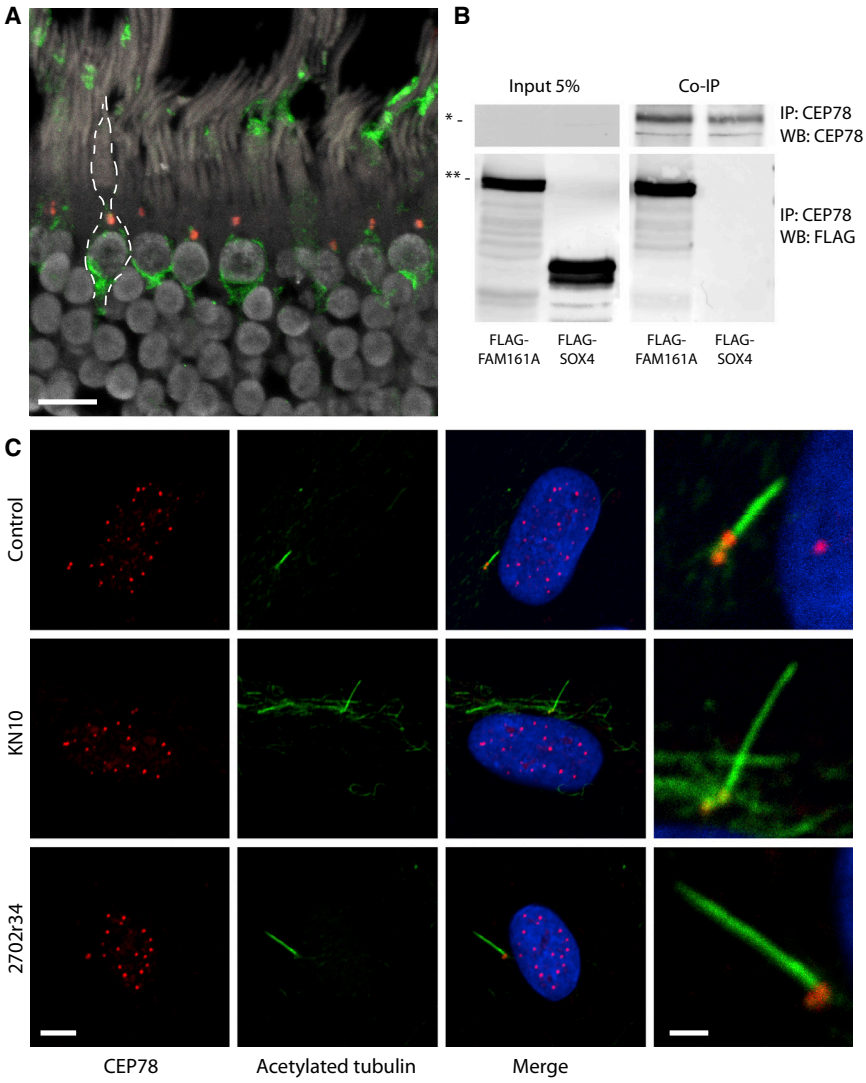

Figure 5. CEP78 in Human Cells and Its Interaction with FAM161A

(A) Immunostaining of CEP78 (red dots) and of cone arrestin (green) in a section of human retina. Margins of a cone photoreceptor are highlighted by a dotted line. The scale bar represents 10 μm.

(B). Co-immunoprecipitation of endogenous CEP78 and FLAG-tagged FAM161A in HEK293T cells. FLAG-SOX4 is a negative control. Abbreviations are as follows: IP:x, protein targeted by the antibody used in immunoprecipitation; and WB:x, protein or peptide targeted by the antibody used in immunoblots. The single and double asterisks indicate the expected molecular sizes for CEP78 (78 kDa) and the FLAG-FAM161A construct (90 kDa), respectively.

(C) Staining of CEP78 (red) and acetylated tubulin (green) in fibroblasts from a control individual, KN10, and 2702r34. CEP78 localizes at the centrioles and at the base of the induced primary cilium. The scale bars represent 5 and 1 μm for regular and magnification panels, respectively.

689) in HEK293T cells transfected with full-length FLAG-FAM161A revealed direct binding between these two ciliary proteins (Figure 5).

On the basis of these findings, we speculated that CRD due to mutations in *CEP78* could be a consequence of hindered ciliary function, similar to what occurs in many other retinal degenerations.[23] To test this hypothesis, we analyzed the morphology of primary cilia in fibroblasts derived from KN10 and 2702r34, with respect to four controls, after serum starvation. Unsupervised counting of at least 82 events per sample (207 events in affected individuals and 430 in controls) revealed that induced cilia in fibroblasts from KN10 and 2702r34 were significantly longer than those from control cells (Figure 6 and Figure S2), a phenomenon that has been previously associated with impaired function of this organelle. For instance, mutations in murine orthologs of *BBS4*, *ICK*, and *TSC1*, linked with ciliopathies such as Bardet-Biedl syndrome, endocrine-cerebro-osteodysplasia, and tuberous sclerosis, respectively, display kidney cells with elongated primary cilia.[24–26]

In recent years, a significant number of hereditary conditions have been recognized to be the consequence of abnormalities of the cellular cilium. These diseases, collectively called ciliopathies, form a genetically heterogeneous spectrum of disorders affecting various tissues and organs, for instance kidney, cochlea, brain, and retina.[23,27] Classical examples of ciliopathies involving retina and other tissues are Usher syndrome (MIM: 276900, blindness and deafness) and Bardet-Biedl syndrome (BBS [MIM: 209900], blindness and multi-organ defects) for both of which vision loss is due to retinitis pigmentosa.[28] In addition, syndromic ciliopathies such as Senior–Løken syndrome (SLS [MIM: 266900]), Joubert syndrome (JBTS [MIM: 213300]), and Jeune syndrome (JATD [MIM: 616300]) can occasionally be accompanied by retinal dystrophy and, in particular, retinitis pigmentosa and/or Leber congenital amaurosis (LCA [MIM: 204000]).[29–32] Another multi-organ ciliopathy is Alström syndrome (ALMS [MIM: 203800]),[33] caused by null mutations in the gene *ALMS1* (MIM: 606844). This disease is characterized by cone-rod degeneration, dilated cardiomyopathy, obesity, type 2 diabetes, and short stature, which can be accompanied by hepatosteatosis and defects in the lungs, kidney, and bladder.[33,34] Most cases also display progressive sensorineural hearing loss.[35] Of interest, mutations in *ALMS1* have recently been suggested as being causative of non-syndromic CRD.[36]

In this study, we show that mutations in *CEP78* result in cone-rod degeneration associated with hearing loss,

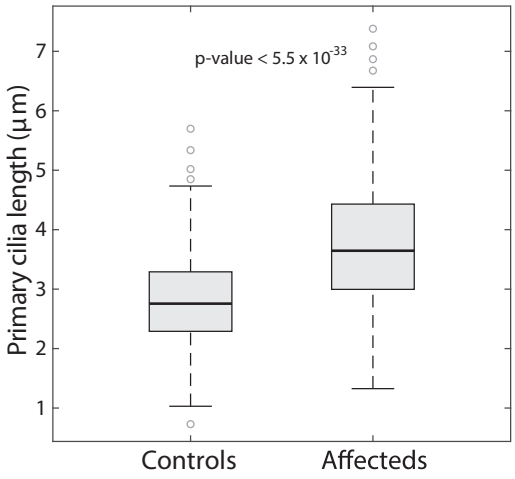

Figure 6. Analysis of Ciliary Lengths
Fibroblasts from affected subjects display significantly longer primary cilia than those from four unaffected controls, suggesting impaired functionality.

another hallmark of ciliopathy, but no other syndromic features. Interestingly, the two Swedish affected individuals had declared hearing loss, and the Greek subject had borderline hearing impairment. An intriguing possibility involves the presence of a genotype-phenotype correlation between *CEP78* alleles and hearing (but not vision), as it is the case for instance for mutations in *USH2A* and *ALMS1*.[36–38] Taken together, our data indicate that genetic defects in *CEP78* define a newly recognized ciliopathy, distinct from Usher and Alström syndromes, affecting both the visual and the hearing systems.

Accession Numbers

The mutations reported in this paper have been deposited in the Leiden Open Variation Database (LOVD) under variant ID numbers 0000119260, 0000119261, and 0000119262.

Supplemental Data

Supplemental Data include two figures and three tables and are available with this article online at http://dx.doi.org/10.1016/j.ajhg.2016.07.009.

Acknowledgments

This work was supported by the Swiss National Science Foundation (grant #156260, to C.R.), by the European Community's Seventh Framework Programmes FP7/2009 under grant agreement #241955 (SYSCILIA) to R.R. and M.U., by the Netherlands Organization for Scientific Research (NWO Vici-865.12.005 to R.R), and by the Rotterdamse Stichting Blindenbelangen, the Stichting Blindenhulp, the Stichting A.F. Deutman Researchfonds Oogheelkunde, and the Stichting voor Ooglijders (to F.P.M.C. and M.I.K.). F.P.M.C. and M.I.K. were also supported by the following foundations: the Algemene Nederlandse Vereniging ter Voorkoming van Blindheid, the Landelijke Stichting voor Blinden en Slechtzienden, the Stichting Retina Nederland Fonds, and the Novartis fund, contributed through UitZicht. We would also like to acknowledge Drs. Andrea Superti-Furga and Luisa Bonafé from the Center for Molecular Diseases of the Lausanne University Hospital, Dr. Frauke Coppieters from the Ghent University Hospital, Dr. Guy Van Camp from the University of Antwerp, and Dr. Isabelle Schrauwen from the Translational Genomics Research Institute in Phoenix.

Received: March 17, 2016
Accepted: July 7, 2016
Published: September 1, 2016

Web Resources

1000 Genomes, http://browser.1000genomes.org
ExAC Browser, http://exac.broadinstitute.org/
GenBank, http://www.ncbi.nlm.nih.gov/genbank/
Leiden Open Variation Database (LOVD), http://www.lovd.nl/3.0/home
NHLBI Exome Sequencing Project (ESP) Exome Variant Server, http://evs.gs.washington.edu/EVS/
OMIM, http://www.omim.org/
RefSeq, http://www.ncbi.nlm.nih.gov/RefSeq
RetNet, https://sph.uth.edu/retnet/

References

1. Hamel, C.P. (2007). Cone rod dystrophies. Orphanet J. Rare Dis. *2*, 7.
2. Berson, E.L., Gouras, P., and Gunkel, R.D. (1968). Progressive cone-rod degeneration. Arch. Ophthalmol. *80*, 68–76.
3. Krauss, H.R., and Heckenlively, J.R. (1982). Visual field changes in cone-rod degenerations. Arch. Ophthalmol. *100*, 1784–1790.
4. Berson, E.L. (1993). Retinitis pigmentosa. The Friedenwald Lecture. Invest. Ophthalmol. Vis. Sci. *34*, 1659–1676.
5. Berger, W., Kloeckener-Gruissem, B., and Neidhardt, J. (2010). The molecular basis of human retinal and vitreoretinal diseases. Prog. Retin. Eye Res. *29*, 335–375.
6. Roosing, S., Thiadens, A.A., Hoyng, C.B., Klaver, C.C., den Hollander, A.I., and Cremers, F.P. (2014). Causes and consequences of inherited cone disorders. Prog. Retin. Eye Res. *42*, 1–26.
7. Royer-Bertrand, B., Castillo-Taucher, S., Moreno-Salinas, R., Cho, T.J., Chae, J.H., Choi, M., Kim, O.H., Dikoglu, E., Campos-Xavier, B., Girardi, E., et al. (2015). Mutations in the heat-shock protein A9 (HSPA9) gene cause the EVEN-PLUS syndrome of congenital malformations and skeletal dysplasia. Sci. Rep. *5*, 17154.
8. Cruickshanks, K.J., Wiley, T.L., Tweed, T.S., Klein, B.E., Klein, R., Mares-Perlman, J.A., and Nondahl, D.M.; The Epidemiology of Hearing Loss Study (1998). Prevalence of hearing loss in older adults in Beaver Dam, Wisconsin. Am. J. Epidemiol. *148*, 879–886.
9. Jerger, J., Chmiel, R., Stach, B., and Spretnjak, M. (1993). Gender affects audiometric shape in presbyacusis. J. Am. Acad. Audiol. *4*, 42–49.
10. Reese, M.G., Eeckman, F.H., Kulp, D., and Haussler, D. (1997). Improved splice site detection in Genie. J. Comput. Biol. *4*, 311–323.
11. Desmet, F.O., Hamroun, D., Lalande, M., Collod-Béroud, G., Claustres, M., and Béroud, C. (2009). Human Splicing Finder: an online bioinformatics tool to predict splicing signals. Nucleic Acids Res. *37*, e67.

12. Hentze, M.W., and Kulozik, A.E. (1999). A perfect message: RNA surveillance and nonsense-mediated decay. Cell *96*, 307–310.
13. Zhang, S.S., Xu, X., Liu, M.G., Zhao, H., Soares, M.B., Barnstable, C.J., and Fu, X.Y. (2006). A biphasic pattern of gene expression during mouse retina development. BMC Dev. Biol. *6*, 48.
14. Schrauwen, I., Hasin-Brumshtein, Y., Corneveaux, J.J., Ohmen, J., White, C., Allen, A.N., Lusis, A.J., Van Camp, G., Huentelman, M.J., and Friedman, R.A. (2016). A comprehensive catalogue of the coding and non-coding transcripts of the human inner ear. Hear. Res. *333*, 266–274.
15. Andersen, J.S., Wilkinson, C.J., Mayor, T., Mortensen, P., Nigg, E.A., and Mann, M. (2003). Proteomic characterization of the human centrosome by protein correlation profiling. Nature *426*, 570–574.
16. Jakobsen, L., Vanselow, K., Skogs, M., Toyoda, Y., Lundberg, E., Poser, I., Falkenby, L.G., Bennetzen, M., Westendorf, J., Nigg, E.A., et al. (2011). Novel asymmetrically localizing components of human centrosomes identified by complementary proteomics methods. EMBO J. *30*, 1520–1535.
17. Azimzadeh, J., Wong, M.L., Downhour, D.M., Sánchez Alvarado, A., and Marshall, W.F. (2012). Centrosome loss in the evolution of planarians. Science *335*, 461–463.
18. Han, Y., Hong, L., Zhong, C., Chen, Y., Wang, Y., Mao, X., Zhao, D., and Qiu, J. (2012). Identification of new altered genes in rat cochleae with noise-induced hearing loss. Gene *499*, 318–322.
19. Bandah-Rozenfeld, D., Mizrahi-Meissonnier, L., Farhy, C., Obolensky, A., Chowers, I., Pe'er, J., Merin, S., Ben-Yosef, T., Ashery-Padan, R., Banin, E., and Sharon, D. (2010). Homozygosity mapping reveals null mutations in *FAM161A* as a cause of autosomal-recessive retinitis pigmentosa. Am. J. Hum. Genet. *87*, 382–391.
20. Langmann, T., Di Gioia, S.A., Rau, I., Stöhr, H., Maksimovic, N.S., Corbo, J.C., Renner, A.B., Zrenner, E., Kumaramanickavel, G., Karlstetter, M., et al. (2010). Nonsense mutations in *FAM161A* cause RP28-associated recessive retinitis pigmentosa. Am. J. Hum. Genet. *87*, 376–381.
21. Di Gioia, S.A., Letteboer, S.J., Kostic, C., Bandah-Rozenfeld, D., Hetterschijt, L., Sharon, D., Arsenijevic, Y., Roepman, R., and Rivolta, C. (2012). FAM161A, associated with retinitis pigmentosa, is a component of the cilia-basal body complex and interacts with proteins involved in ciliopathies. Hum. Mol. Genet. *21*, 5174–5184.
22. Di Gioia, S.A. (2013). Targeted sequence capture and ultra high throughput sequencing for gene discovery in inherited diseases. PhD Thesis (University of Lausanne, Lausanne, Switzerland).
23. Wright, A.F., Chakarova, C.F., Abd El-Aziz, M.M., and Bhattacharya, S.S. (2010). Photoreceptor degeneration: Genetic and mechanistic dissection of a complex trait. Nat. Rev. Genet. *11*, 273–284.
24. Armour, E.A., Carson, R.P., and Ess, K.C. (2012). Cystogenesis and elongated primary cilia in *Tsc1*-deficient distal convoluted tubules. Am. J. Physiol. Renal Physiol. *303*, F584–F592.
25. Moon, H., Song, J., Shin, J.O., Lee, H., Kim, H.K., Eggenschwiller, J.T., Bok, J., and Ko, H.W. (2014). Intestinal cell kinase, a protein associated with endocrine-cerebro-osteodysplasia syndrome, is a key regulator of cilia length and Hedgehog signaling. Proc. Natl. Acad. Sci. USA *111*, 8541–8546.
26. Mokrzan, E.M., Lewis, J.S., and Mykytyn, K. (2007). Differences in renal tubule primary cilia length in a mouse model of Bardet-Biedl syndrome. Nephron, Exp. Nephrol. *106*, e88–e96.
27. Waters, A.M., and Beales, P.L. (2011). Ciliopathies: An expanding disease spectrum. Pediatr. Nephrol. *26*, 1039–1056.
28. Koenig, R. (2003). Bardet-Biedl syndrome and Usher syndrome. Dev. Ophthalmol. *37*, 126–140.
29. Bachmann-Gagescu, R., Dempsey, J.C., Phelps, I.G., O'Roak, B.J., Knutzen, D.M., Rue, T.C., Ishak, G.E., Isabella, C.R., Gorden, N., Adkins, J., et al.; University of Washington Center for Mendelian Genomics (2015). Joubert syndrome: a model for untangling recessive disorders with extreme genetic heterogeneity. J. Med. Genet. *52*, 514–522.
30. Bard, L.A., Bard, P.A., Owens, G.W., and Hall, B.D. (1978). Retinal involvement in thoracic-pelvic-phalangeal dystrophy. Arch. Ophthalmol. *96*, 278–281.
31. Wilson, D.J., Weleber, R.G., and Beals, R.K. (1987). Retinal dystrophy in Jeune's syndrome. Arch. Ophthalmol. *105*, 651–657.
32. Hildebrandt, F., and Zhou, W. (2007). Nephronophthisis-associated ciliopathies. J. Am. Soc. Nephrol. *18*, 1855–1871.
33. Marshall, J.D., Muller, J., Collin, G.B., Milan, G., Kingsmore, S.F., Dinwiddie, D., Farrow, E.G., Miller, N.A., Favaretto, F., Maffei, P., et al. (2015). Alström syndrome: Mutation spectrum of *ALMS1*. Hum. Mutat. *36*, 660–668.
34. Marshall, J.D., Maffei, P., Collin, G.B., and Naggert, J.K. (2011). Alström syndrome: genetics and clinical overview. Curr. Genomics *12*, 225–235.
35. Marshall, J.D., Bronson, R.T., Collin, G.B., Nordstrom, A.D., Maffei, P., Paisey, R.B., Carey, C., Macdermott, S., Russell-Eggitt, I., Shea, S.E., et al. (2005). New Alström syndrome phenotypes based on the evaluation of 182 cases. Arch. Intern. Med. *165*, 675–683.
36. Lazar, C.H., Kimchi, A., Namburi, P., Mutsuddi, M., Zelinger, L., Beryozkin, A., Ben-Simhon, S., Obolensky, A., Ben-Neriah, Z., Argov, Z., et al. (2015). Nonsyndromic early-onset cone-rod dystrophy and limb-girdle muscular dystrophy in a consanguineous Israeli family are caused by two independent yet linked mutations in *ALMS1* and *DYSF*. Hum. Mutat. *36*, 836–841.
37. Rivolta, C., Sweklo, E.A., Berson, E.L., and Dryja, T.P. (2000). Missense mutation in the *USH2A* gene: association with recessive retinitis pigmentosa without hearing loss. Am. J. Hum. Genet. *66*, 1975–1978.
38. Lenassi, E., Vincent, A., Li, Z., Saihan, Z., Coffey, A.J., Steele-Stallard, H.B., Moore, A.T., Steel, K.P., Luxon, L.M., Héon, E., et al. (2015). A detailed clinical and molecular survey of subjects with nonsyndromic USH2A retinopathy reveals an allelic hierarchy of disease-causing variants. Eur. J. Hum. Genet. *23*, 1318–1327.

The American Journal of Human Genetics, Volume *99*

Supplemental Data

Mutations in *CEP78* Cause Cone-Rod Dystrophy and Hearing Loss Associated with Primary-Cilia Defects

Konstantinos Nikopoulos, Pietro Farinelli, Basilio Giangreco, Chrysanthi Tsika, Beryl Royer-Bertrand, Martial K. Mbefo, Nicola Bedoni, Ulrika Kjellström, Ikram El Zaoui, Silvio Alessandro Di Gioia, Sara Balzano, Katarina Cisarova, Andrea Messina, Sarah Decembrini, Sotiris Plainis, Styliani V. Blazaki, Muhammad Imran Khan, Shazia Micheal, Karsten Boldt, Marius Ueffing, Alexandre P. Moulin, Frans P.M. Cremers, Ronald Roepman, Yvan Arsenijevic, Miltiadis K. Tsilimbaris, Sten Andréasson, and Carlo Rivolta

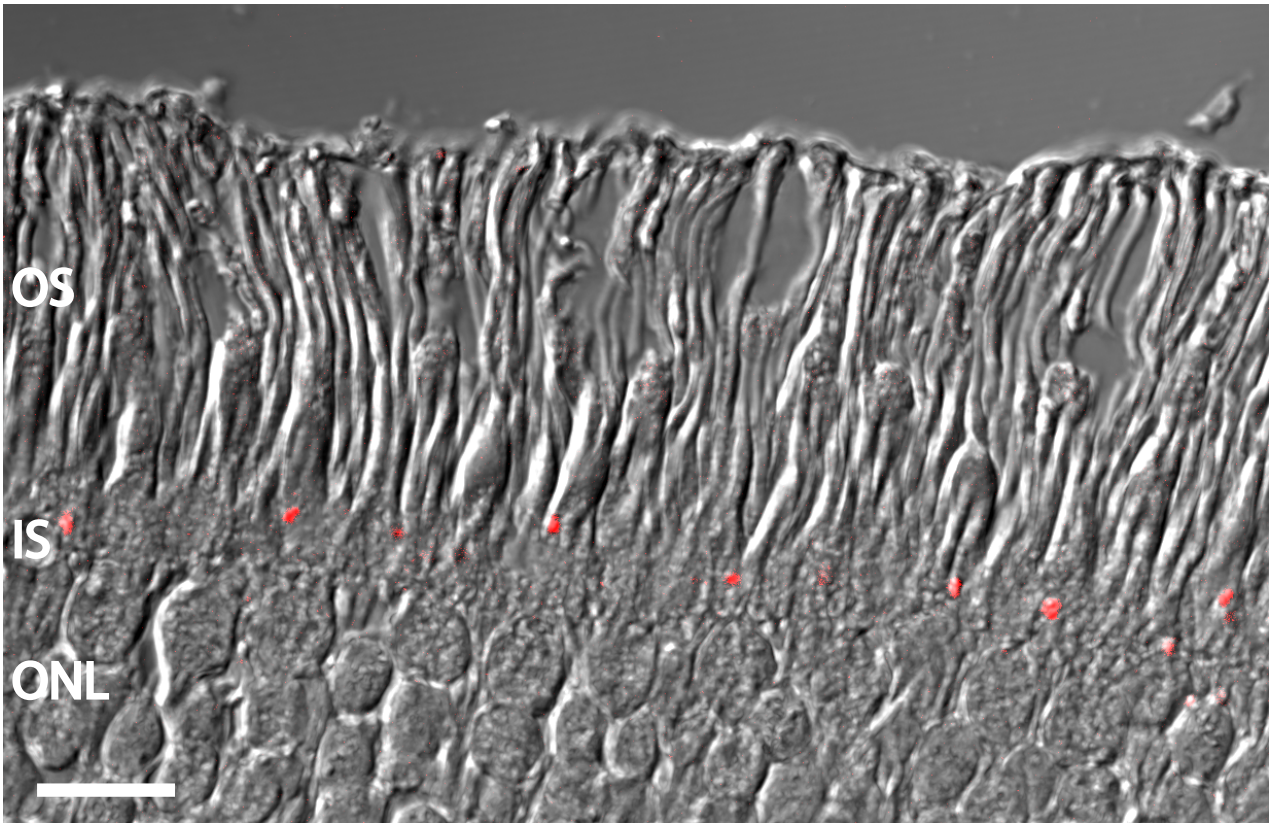

Figure S1. Immunostaining of CEP78 in a section of human retina (red dots) reveals its presence in the inner segment (IS) of photoreceptors, likely at the base of the connecting cilium. OS, outer segments; ONL, outer nuclear layer. Scale bar: 10 µm.

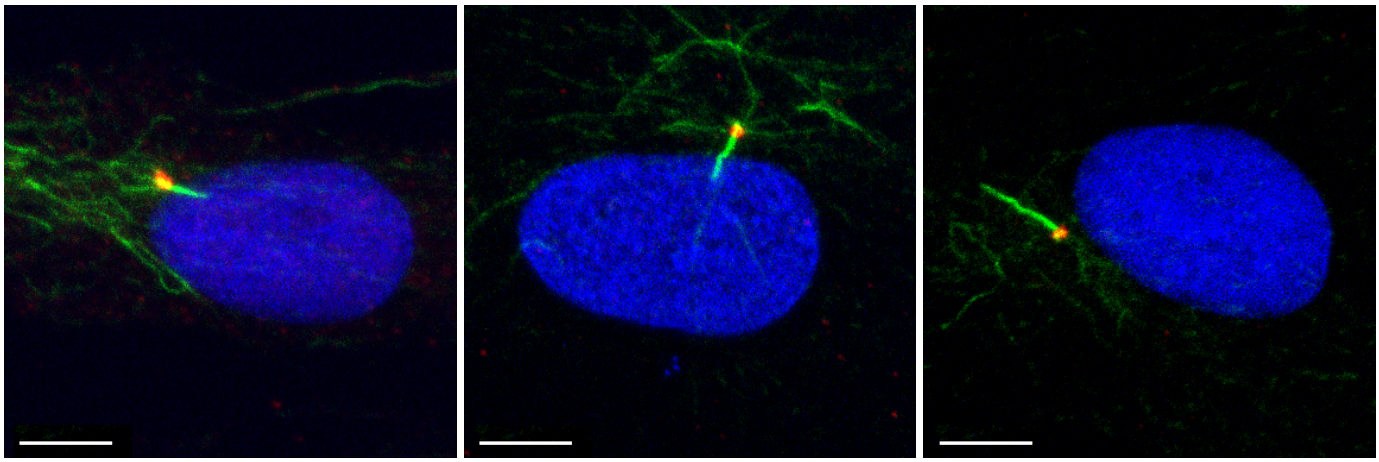

Control KN10 2702r34

Figure S2: Representative samples of the images used for the analysis of cilia lengths, displayed in Figure 6. Green, acetylated tubulin, marking the ciliary axoneme; red, ninein, marking the base of the cilium. Scale bar: 5 µm.

Patient	KN10	2716s15
Number of exonic and splicing variants	22,956	22,299
Number of non-synonymous variants	11,347	11,012
Number of rare variants (<1%)	663	527
Number of rare variants after quality control (QC)	335	212
Number of genes with homozygous variants	7	3
Number of genes with 2 heterozygous variants	15	7
Genes in common	*CEP78* and *TTN*	

Table S1. Overview of exonic and splicing variants observed in the two patients, following sequential filtering procedures. Values refer to number of variants unless specified otherwise. Rare (<1%): Variant frequency = 1% or less in public databases – ExAC, ESP, and Wellderly, 1KG (from Complete Genomics). QC: Rare variants after quality control, i.e. after removal of (1) WES data of poor quality, with less than 15 reads per nucleotide and genotype quality less than 50, (2) variants present in control WES processed by the same pipeline (to remove any technical errors), and (3) variants carried by healthy homozygous individuals in public database (e.g. ExAC). The gene *TTN* appears frequently as a false positive finding in WES studies.

Table S2. Genes with rare homozygous or compound heterozygous variants

ID	Var_type	gene	chr	begin	end	ref	alt	zyg	rs
KN10	nonsynonymous SNV	NPR1	chr1	153658297	153658298	G	A	hom	rs61757359
KN10	nonsynonymous SNV	F8	chrX	154182235	154182236	C	T	hom	.
KN10	nonsynonymous SNV	CHDC2	chrX	36091352	36091353	T	A	hom	.
KN10	nonsynonymous SNV	GPR112	chrX	135496331	135496332	G	A	hom	rs201992547
KN10	nonsynonymous SNV	PCDH11X	chrX	91133925	91133926	G	T	hom	.
KN10	splicing	CEP78	chr9	80855281	80855282	G	T	hom	.
KN10	nonsynonymous SNV	AKAP4	chrX	49958477	49958478	C	T	hom	rs141513690
KN10	splicing	SKA3	chr13	21746644	21746691	C	CGCTTTCC	het	.
KN10	nonsynonymous SNV	SKA3	chr13	21729945	21729946	T	A	het	.
KN10	nonsynonymous SNV	DCHS2	chr4	155241752	155241753	C	T	het	.
KN10	nonsynonymous SNV	DCHS2	chr4	155411721	155411722	G	A	het	rs199621086
KN10	nonsynonymous SNV	TTN	chr2	179406044	179406045	C	T	het	rs55704830
KN10	nonsynonymous SNV	TTN	chr2	179529441	179529442	C	G	het	.
KN10	nonsynonymous SNV	TTN	chr2	179578857	179578858	G	A	het	rs72648990
KN10	nonsynonymous SNV	TTN	chr2	179602948	179602949	G	T	het	rs55906845
KN10	nonsynonymous SNV	MUC2	chr11	1092884	1092885	C	T	het	rs201415503
KN10	nonframeshift deletion	MUC2	chr11	1093438	1093439	GTGACCCC	G	het	.
KN10	nonsynonymous SNV	MUC2	chr11	1093531	1093532	A	G	het	rs56104295
KN10	nonsynonymous SNV	MUC2	chr11	1093549	1093550	G	C	het	rs79238439
KN10	nonsynonymous SNV	MUC2	chr11	1093550	1093551	T	C	het	rs55941874
KN10	nonsynonymous SNV	MUC2	chr11	1093555	1093556	C	T	het	.
KN10	nonsynonymous SNV	MUC2	chr11	1093591	1093592	A	C	het	rs200739161
KN10	nonsynonymous SNV	MUC2	chr11	1093619	1093620	T	C	het	.
KN10	nonsynonymous SNV	PPCS	chr1	42922318	42922319	G	A	het	.
KN10	nonsynonymous SNV	PPCS	chr1	42922319	42922320	C	A	het	.
KN10	nonsynonymous SNV	ABCA2	chr9	139907306	139907307	C	T	het	.
KN10	nonframeshift deletion	ABCA2	chr9	139908757	139908758	TGGGTCAC	T	het	.
KN10	nonsynonymous SNV	ABCB6	chr2	220075811	220075812	C	T	het	.
KN10	nonsynonymous SNV	ABCB6	chr2	220077164	220077165	C	T	het	.
KN10	nonsynonymous SNV	TAS2R30	chr12	11286702	11286703	G	C	het	rs113026132
KN10	nonsynonymous SNV	TAS2R30	chr12	11286746	11286747	A	G	het	.
KN10	nonframeshift insertion	NCOR2	chr12	124887058	124887068	G	GGCTGCTC	het	.
KN10	nonsynonymous SNV	NCOR2	chr12	124968176	124968177	G	A	het	.
KN10	nonsynonymous SNV	FAM193B	chr5	176952101	176952102	C	T	het	rs201231555
KN10	nonsynonymous SNV	FAM193B	chr5	176952178	176952179	T	G	het	rs185300146
KN10	frameshift insertion	ANKRD36	chr2	97851231	97851245	A	AACCAAAA	het	.
KN10	frameshift insertion	ANKRD36	chr2	97851233	97851248	T	TGCATCAC	het	.
KN10	nonsynonymous SNV	MUC17	chr7	100678079	100678080	A	T	het	.
KN10	nonsynonymous SNV	MUC17	chr7	100681266	100681267	C	A	het	rs142126972
KN10	nonsynonymous SNV	MUC4	chr3	195512515	195512516	G	T	het	.
KN10	nonsynonymous SNV	MUC4	chr3	195513145	195513146	A	G	het	.
KN10	nonsynonymous SNV	IL1R1	chr2	102782690	102782691	T	C	het	rs34889382
KN10	nonsynonymous SNV	IL1R1	chr2	102791994	102791995	G	A	het	rs34835752
KN10	nonsynonymous SNV	ENAM	chr4	71507930	71507931	G	A	het	.
KN10	nonsynonymous SNV	ENAM	chr4	71510354	71510355	G	C	het	.
2716s15	nonsynonymous SNV	PLAC1	chrX	133700133	133700134	A	G	hom	.
2716s15	nonsynonymous SNV	MAGIX	chrX	49021639	49021640	C	T	hom	rs183982494
2716s15	nonsynonymous SNV	MID1	chrX	10469476	10469477	C	T	hom	rs111428432
2716s15	nonsynonymous SNV	DNAH7	chr2	196636502	196636503	C	G	het	.
2716s15	nonsynonymous SNV	DNAH7	chr2	196726484	196726485	C	T	het	rs201185180
2716s15	frameshift deletion	ZDHHC11	chr5	825327	825328	TAA	T	het	rs66846455
2716s15	nonsynonymous SNV	ZDHHC11	chr5	825331	825332	T	G	het	.
2716s15	frameshift insertion	ZDHHC11	chr5	825333	825336	C	CAT	het	.
2716s15	nonsynonymous SNV	ZDHHC11	chr5	825338	825339	G	A	het	rs2335582
2716s15	nonsynonymous SNV	CDC27	chr17	45219702	45219703	T	C	het	rs199774308
2716s15	nonsynonymous SNV	CDC27	chr17	45219714	45219715	T	G	het	rs77550690
2716s15	nonsynonymous SNV	CDC27	chr17	45219723	45219724	C	G	het	rs77609498
2716s15	nonsynonymous SNV	TOPAZ1	chr3	44285446	44285447	A	G	het	rs17076541
2716s15	nonsynonymous SNV	TOPAZ1	chr3	44286384	44286385	A	G	het	rs17076545
2716s15	nonsynonymous SNV	POMZP3	chr7	76240814	76240815	C	T	het	rs17419421
2716s15	nonsynonymous SNV	POMZP3	chr7	76240819	76240820	C	T	het	rs17341271
2716s15	splicing	TTN	chr2	179563643	179563645	T	TA	het	.
2716s15	nonsynonymous SNV	TTN	chr2	179485184	179485185	T	C	het	.
2716s15	splicing	CEP78	chr9	80855285	80855286	G	A	het	.
2716s15	frameshift deletion	CEP78	chr9	80858405	80858406	AC	A	het	.

Table S3. Cochlear expression (as FPKM) of genes known to be involved in hereditary deafness, and of CEP78

Number	gene_id	gene_name	Coch 1	Coch 2	Coch 3	Average
1	ENSG00000091010.4	POU4F3	0	0	0	0
2	ENSG00000095777.10	MYO3A	0.000635	0.004849	0.022596	0.00936
3	ENSG00000179520.6	SLC17A8	0.000389	0.000547	0.032021	0.010986
4	ENSG00000167210.12	LOXHD1	0.025365	0.060565	0.0066	0.030843
5	ENSG00000179855.5	GIPC3	0.024089	0.076229	0.039106	0.046475
6	ENSG00000181585.3	TMIE	0	0.06341	0.146477	0.069962
7	ENSG00000139304.8	PTPRQ	0.006097	0.112682	0.099155	0.072645
8	ENSG00000167791.7	CABP2	0.040399	0.173213	0.056216	0.089943
9	ENSG00000115155.12	OTOF	0.057953	0.003852	0.223894	0.095233
10	ENSG00000242866.5	STRC	0.12565	0.132264	0.119115	0.125676
11	ENSG00000170615.10	SLC26A5	0.129152	0.092504	0.255584	0.15908
12	ENSG00000176058.7	TPRN	0.094411	0.104095	0.326162	0.174889
13	ENSG00000214756.3	METTL12	0.564632	0.064836	4.28E-32	0.209823
14	ENSG00000187848.8	P2RX2	0.154111	0.470321	0.119013	0.247815
15	ENSG00000155719.12	OTOA	0.00562	0.127403	0.668946	0.267323
16	ENSG00000165091.11	TMC1	0.264026	0.366298	0.209721	0.280015
17	ENSG00000145103.8	ILDR1	0.221374	0.105951	0.538851	0.288725
18	ENSG00000215203.2	GRXCR1	0.012123	0.461481	0.436519	0.303374
19	ENSG00000162399.6	BSND	0.152115	0.492989	0.344713	0.329939
20	ENSG00000117013.10	KCNQ4	0.095	0.904738	0.154929	0.384889
21	ENSG00000187017.10	ESPN	0.194628	0.853735	0.111057	0.386473
22	ENSG00000137474.15	MYO7A	0.52261	0.257552	0.428576	0.402913
23	ENSG00000146038.7	DCDC2	1.67294	0.284403	0.334591	0.763978
24	ENSG00000150275.13	PCDH15	0.253788	1.64893	0.788694	0.897137
25	ENSG00000213892.6	CEACAM16	0.013226	0.570029	2.18102	0.921425
26	ENSG00000169519.15	METTL15	1.24601	0.662215	1.06318	0.990468
27	ENSG00000121957.8	GPSM2	0.283602	1.17825	1.86853	1.110127
28	ENSG00000091536.12	MYO15A	1.31241	1.0893	1.4237	1.275137
29	ENSG00000159261.6	CLDN14	0.123397	0.915213	2.79064	1.276417
30	ENSG00000091137.7	SLC26A4	1.17451	1.33071	1.34425	1.283157
31	ENSG00000109927.5	TECTA	2.24775	1.5015	0.631862	1.460371
32	ENSG00000136425.8	CIB2	2.28468	0.808458	1.45781	1.516983
33	ENSG00000101574.10	METTL4	1.32381	1.23014	2.15561	1.569853
34	ENSG00000160183.9	TMPRSS3	2.1716	1.13005	2.42714	1.909597
35	ENSG00000152939.10	MARVELD2	1.52109	2.19185	2.07644	1.929793
36	ENSG00000155093.13	PTPRN2	1.97559	1.41402	2.79015	2.05992
37	ENSG00000107736.15	CDH23	2.65421	2.50604	1.47115	2.210467
38	ENSG00000019991.11	HGF	1.20093	4.00613	1.92118	2.37608
39	ENSG00000119715.10	ESRRB	1.27515	3.85601	3.7147	2.94862
40	ENSG00000130703.11	OSBPL2	4.65872	4.52819	4.36676	4.51789
41	ENSG00000148019.8	CEP78	4.50804	2.30044	6.7815	4.529993
42	ENSG00000165819.7	METTL3	4.32555	5.5211	4.21988	4.688843
43	ENSG00000165792.13	METTL17	6.26857	3.73464	5.09427	5.032493
44	ENSG00000105928.9	DFNA5	2.09614	3.53489	9.83763	5.15622
45	ENSG00000105357.11	MYH14	5.2459	5.24015	5.54507	5.343707
46	ENSG00000131504.11	DIAPH1	6.75299	6.37873	5.71255	6.281423
47	ENSG00000174099.6	MSRB3	8.75399	4.9088	7.14766	6.936817
48	ENSG00000167815.7	PRDX2	7.68825	5.19914	8.5183	7.13523
49	ENSG00000152492.9	CCDC50	5.48502	8.655	8.96887	7.702963
50	ENSG00000111913.11	FAM65B	9.52451	5.83092	7.94286	7.766097
51	ENSG00000109501.9	WFS1	13.7706	3.90427	6.26541	7.980093
52	ENSG00000147224.6	PRPS1	6.76141	9.64509	7.9225	8.109667
53	ENSG00000100106.15	TRIOBP	8.23531	9.62484	8.07235	8.644167
54	ENSG00000119139.12	TJP2	10.16	11.5985	5.61086	9.12312
55	ENSG00000124570.13	SERPINB6	9.76828	9.82138	8.69881	9.42949
56	ENSG00000196767.4	POU3F4	14.6888	15.8231	20.3449	16.95227
57	ENSG00000105976.10	MET	19.6721	23.953	8.66128	17.42879
58	ENSG00000065427.10	KARS	22.3542	20.2033	24.4067	22.3214
59	ENSG00000126778.7	SIX1	31.1925	21.4469	17.086	23.2418
60	ENSG00000100345.16	MYH9	30.2774	26.0357	16.2673	24.19347
61	ENSG00000112319.13	EYA4	30.046	16.2611	31.7525	26.01987
62	ENSG00000091482.5	SMPX	15.8038	10.495	55.7151	27.33797
63	ENSG00000196586.9	MYO6	28.8111	32.6395	35.8846	32.44507
64	ENSG00000006611.11	USH1C	30.8977	21.6356	50.2302	34.2545
65	ENSG00000137710.10	RDX	57.7042	35.1006	32.5633	41.78937
66	ENSG00000151491.8	EPS8	49.8291	34.1867	44.4353	42.81703
67	ENSG00000121742.11	GJB6	157.935	24.7138	78.0029	86.8839
68	ENSG00000204248.6	COL11A2	133.261	88.6713	257.319	159.7504
69	ENSG00000165474.5	GJB2	384.907	81.9362	257.936	241.5931
70	ENSG00000184009.5	ACTG1	808.74	427.013	462.764	566.1723
71	ENSG00000100473.11	COCH	3679.96	819.586	4595.38	3031.642

Data from: https://www.tgen.org/home/research/research-divisions/neurogenomics/supplementary-data/inner-ear-transcriptome.aspx